Thermal Science and Engineering (2020) Volume 3 Issue 2
doi:10.24294/tse.v3i2.1500

ORIGINAL RESEARCH ARTICLE

Equilibrium, thermodynamics and kinetic models in the adsorption of Red 40 on corn gourd

Danilo Figueroa*, Anderson Moreno, Angelina Hormaza

Escuela de Química, Facultad de Ciencias, Universidad Nacional de Colombia - Sede Medellín, Colombia. E-mail: dfigueroap@unal.edu.co

ABSTRACT

Adsorption is a widely used method for the treatment of dissolved contaminants. Various agro-industrial wastes have been explored as potential adsorbents, showing high efficiency in dye removal. Each adsorbate-adsorbent pair needs kinetic, and equilibrium models to scale up this process. In this work, the equilibrium, kinetics and thermodynamics of the corn Tuza-Red 40 system were evaluated under batch system at pH = 2.0 at temperatures of 25, 40, and 55 °C. The Langmuir, Freundlich and Temkin models were selected for the isotherm representation, while the Lagergren, Ho, and Elovich equations for the kinetics of the process. The Freundlich model presented the best fit to the isotherms, the adsorption kinetics was best described by the Ho equation, and the values for Gibbs free energy and entropy indicated the spontaneity and feasibility of the process.

Keywords: Adsorption Isotherms; Kinetics; Red 40; Low-cost Adsorbents; Corn Stover

ARTICLE INFO

Received: 29 June 2020
Accepted: 22 August 2020
Available online: 1 September 2020

1. Introduction

O The exact amount of synthetic dyes produced in the world is unknown; commercially there are more than 100,000 varieties and it has been estimated a production of about 7 × 105 to 1 × 106 tons per year[1]. The precise amount of dyes discharged into the environment is also unknown, but it has been reported that in their production process, as well as in industrial applications, a value of approximately 10%–15% is discharged untreated into the environment[2].

Azo dyes and their pigments are considered to be the largest chemical group of the currently existing ones, about 26,000 dyes. The azo group has been found by animal testing to cause cancer; therefore, its carcinogenic effect on humans is expected[3]. To this group belongs the dye red 40 (R40), known as Allura red and commonly used as a dye in food, beverages and tattoos[4]. Minimal amounts, even of 1 ppm of dye, are sufficient to cause an aesthetic deterioration of the environment[5]. However, the most drastic repercussion of its presence is verified in the photosynthetic processes, where a reduction in the penetration of solar radiation prevents the processes of self-regeneration of the water resource, affecting the aquatic biota[6].

The release of considerable quantities of synthetic dyes into the environment has caused public interest, legislation problems and a serious challenge for environmental scientists. In addition, the social trend for the growth of environmental protection and preservation of natural resources promotes the promotion of industrial technologies with lower environmental impact, which reduce water consumption and reduce the discharge of highly colored effluents[1].

Among the non-traditional treatment methods is adsorption, where the dye is retained on the surface of an adsorbent material to obtain a decolorized effluent. Activated carbon is widely used as an adsorbent, but it has a narrow polarity range that prevents the removal of some dyes. Moreover, it can be regenerated after each operating cycle, but this leads to losses of up to 10% of the adsorbent material. On the other hand, its production and regeneration demand a large amount of energy, which limits its use in the treatment of colored effluents due to its high cost[7-8].

Maize is one of the crops with the highest production in the world and generates agricultural residues such as trash (TM), leaf, and bagasse, which are incinerated in a large proportion[9]. TM is, therefore, a renewable, available, and low-cost agricultural by-product, for which dye and heavy metal adsorption capacities have been reported for both native and modified material, pointing to its alternative use as a potential adsorbent[7,10].

The purpose of this work is to evaluate the adsorptive capacity of the anionic dye R40 on TM through different isotherms, as well as the speed of the process through its kinetics, as fundamental parameters required for its design on a larger scale.

2. Materials and methods

2.1 Adsorbent preparation

Obtain the agricultural residue TM from a local market in the city. Its preparation included the first rinse with potable water, air-drying and size reduction with a blade mill, and selecting a particle size by sieving between 0.30 and 0.71 mm. Subsequently, wash it with distilled water and hydrogen peroxide solution not until obtaining a material free of organic material. Then dry it at a temperature of 80 °C for 24 h in a forced convection oven. Finally, the material was hermetically stored, periodically controlling the humidity with the ADAM humidity analyzer.

2.2 Preparation of the R40 solution and its quantification

Commercial R40 dye is obtained from local industry. Its solution was prepared in a 250 mL volumetric balloon with 250 mg of this dye and deionized water, maintaining agitation for 15 min. Measure the concentration through the Perkin-Elmer Lambda 35 Uv-Vis spectrophotometer at $\lambda_{max} = 502$ nm. It should be noted that a calibration curve was previously performed with concentrations between 2.0 and 40 $mg \cdot L^{-1}$ of R40 to achieve a fit of $R^2 = 0.999$. Set the pH of the solution was to a value of 2.0 with a 0.1 N concentration HCL solution.

2.3 Tests for thermodynamic studies

In a 100 mL glass vessel, 10 mL of the R40 solution diluted to a concentration between 5.0 and 40 $mg \cdot L^{-1}$ were deposited, with a TM dosage of 5.8 $g \cdot L^{-1}$, maintaining a constant agitation of 120 rpm. Each assay was carried out at the temperature of 25, 40, and 55 °C in a Heidolph shaker equipped with temperature control. After three h of duration, an aliquot was taken, centrifuged and the supernatant concentration was measured.

2.4 Assays for kinetic studies

In glass containers, 10 mL of the R40 dye solution prepared at a concentration of 10 $mg \cdot L^{-1}$ were taken, with a TM dosage of 5.8 $g \cdot L^{-1}$, maintaining a constant agitation of 120 rpm (these values were selected as a result of a previous experimental design that achieved dye removals greater than 98%). Each test was carried out at a temperature of 25, 40 and 55 °C, where the samples were quantified sequentially during a period of 150 min. For each analysis, the sample and two replicates were prepared, respectively, taking aliquots of 1.5 ml.

2.5 Thermodynamic and kinetic studies

The analysis of adsorption data is important for the development of equilibrium and kinetic equations that can be used for design purposes. When considering dilute solutions of the dye, it is assumed that the solution volume remains constant during the process or evaporation losses are negligible; the loading of adsorbed dye R40 per mass of adsorbent TM is quantified by Equation 1.

$$q_t = (C_0 - C_t)\frac{V}{W} \tag{1}$$

Where, C_0 is the initial concentration of the solution (mg·L^{-1}), C_t is the concentration at an instant *t* once the process has started, *V* is the volume of the solution (L) and W is the dosage of TM (g). Therefore, we express q_t as the adsorbed mass of R40 per mass of TM (mg·g^{-1}) at a given instant. If the duration of the process is long enough to reach equilibrium, there will be q_t, and it be constant to be called q_e, charge at equilibrium corresponding to the concentration at equilibrium C_e, forming the respective pair of equilibrium data[11].

2.5.1 Adsorption equilibrium

The details of the process equilibrium, generally known as adsorption isotherms, describe the behavior of the adsorbate-adsorbent interaction and provide information on the capacity of the adsorbent under study. Three models, Langmuir, Freundlich and Temkin, each with two characteristic constants, are studied for this R40-TM adsorption system[11-13].

The Langmuir isotherm is a valid theoretical model for adsorption in a monolayer on a completely homogeneous surface with a finite number of identical and specific adsorption sites and with negligible interaction between molecules, represented by Equation 2.

$$q_e = \frac{q_{max} K_L C_e}{1 + K_L C_e} \tag{2}$$

Where, the parameter q_{max}(mg·g^{-1}) is a constant that denotes the maximum adsorption capacity, while the constant K_L (L·mg^{-1}) defines the affinity of the adsorbate for the adsorbent.

The Freundlich model is an empirical equation that assumes no homogeneity in the energy of the sites on the surface and no limit on the maximum adsorption load, and shows a consistency of an exponential distribution of active centers characteristic of a heterogeneous surface, represented as Equation 3.

$$q_e = K_F C_e^{1/n} \tag{3}$$

The parameters K_F (mg·g^{-1} (mg·L^{-1})$^{-1/n}$) and *n* characterize the adsorption capacity and intensity, respectively; hypothetically K_F reaches the value of q_e when C_e approaches unity and thus can be considered as an indicator of adsorption intensity.

The Temkin Model, characterized by a uniform distribution of binding energy, up to a certain maximum binding energy, introduces constants whose values depend on the initial heat of adsorption and assumes a linear decrease of the heat of adsorption with the degree of coating, expressed in Equation 4.

$$q_e = B \ln(AC_e) \tag{4}$$

Where, *B* is a constant that is related to the heat of adsorption and *A* (L·mg^{-1}) is the equilibrium binding constant corresponding to the maximum binding energy.

2.5.2 Thermodynamic parameters

The thermodynamic parameters reflect the feasibility and spontaneous nature of the process; thus, the free energy change, enthalpy change and surface entropy change can be estimated using the change of the equilibrium constant with absolute temperature. The heterogeneous equilibrium that is reached can be represented by the apparent equilibrium constant K_c' defined by Equation 5.

$$K_c' = \frac{C_{ad,e}}{C_e} \tag{5}$$

Where, $C_{ad,e}$ is the concentration of the adsorbed dye on the adsorbent, and considering the adsorbent dose in g·L^{-1}, the value of $C_{ad,e}$ will be the value of q_e, different values of the apparent constant are obtained for each pair of data but those values corresponding to the most dilute concentrations are selected. Hypothetically extrapolating the concentration to zero, the value of the apparent constant will be taken as the standard equilibrium constant K_c^0 of the adsorption system, particularly with the Langmuir isotherm one can calculate K_c^0 as $q_{\max} \times K_L$. The value of K_c^0 the change in adsorption free energy ΔG° (kJ·mol^{-1}) at the respective temperature is measured. R is the universal gas constant (8.314 J·mol^{-1}·K^{-1}), and T (K) is the absolute temperature. The change in free energy indicates the degree of spontaneity of the process. More negative values reflect a greater favorability of adsorption, and its variation can be expressed as a function of the change in enthalpy ΔH° (kJ·mol^{-1}) and entropy ΔS° (J·mol^{-1}·K^{-1}) of adsorption with temperature, obtaining the regression line with slope ΔS° and intercept ΔH°, as shown in Equation 7.

$$\Delta G^{\circ} = \Delta H^{\circ} - T\Delta S^{\circ} \tag{6}$$

A negative value of ΔH° reflects that the process is exothermic in nature, while negative values of ΔS° indicate a decrease in randomness at the solution-solid interface during adsorption[2,14].

2.5.3 Adsorption kinetics

In adsorption, as a time-dependent process, it is necessary to know its speed for the design and evaluation of adsorbents. Two criteria are used to represent adsorption kinetic models: the concentration of the solution or the loading on the adsorbent. Generally, the pseudo-first-order Lagergren, pseudo-second-order Ho and Elovich models have been commonly used as simplified models in adsorption dynamics[2,9,11].

Lagergren's pseudo-first-order model is described mathematically by Equation 8.

$$\frac{dq_t}{dt} = K_1\left(q_e - q_t\right) \tag{7}$$

Where, K_1 (min^{-1}) is the first order adsorption kinetic constant, and q_e is the dye loading at equilibrium, where this parameter must be previously established before determining the model fit, considering the adsorbent initially free of solute, i.e., under the boundary conditions $t = 0$ with $q_t = 0$, $t = t$, $q_t = q_t$, in an integrated form we have Equation 9.

$$q_t = q_e\left(1 - e^{-K_1 t}\right) \tag{8}$$

The pseudo-second-order Ho model, this model is usually attributed to the process involving a chemisorption mechanism. It is noteworthy for its particularity in estimating the equilibrium load, as shown in Equation 10.

$$\frac{dq_t}{dt} = K_2\left(q_e - q_t\right)^2 \tag{9}$$

Where, K_2 $\left(g \cdot \mathrm{mg}^{-1} \cdot \mathrm{min}^{-1}\right)$ is the second-order adsorption kinetic constant, whose integration under the same boundary conditions, previously described, is represented by Equation 11.

$$q_t = \frac{K_2 q_e^2 t}{1 + K_2 q_e t} \tag{10}$$

The Elovich model, of general application in chemisorption processes, assumes that the adsorbent active sites are heterogeneous and thus exhibit different activation energies, based on a second order reaction mechanism for a heterogeneous reaction process, described mathematically in Equation 12.

$$\frac{dq_t}{dt} = \alpha e^{-\beta q_t} \tag{11}$$

Where, α $\left(g \cdot \mathrm{mg}^{-1} \cdot \mathrm{min}^{-1}\right)$ is the initial adsorption velocity, β is related to the surface area covered, and chemisorption activation energy. It is represented in Equation 13.

$$q_t = \frac{1}{\beta}\ln\left(\beta\alpha t\right) \tag{12}$$

2.5.4 Activation energy

The adsorption activation energy E_a (kJmol^{-1}) was calculated by Equation 14, in the linearized Arrhenius form:

$$\ln K = \ln A - \left(E_a / RT\right) \tag{13}$$

Where, the value K is the kinetic constant that controls the process at the absolute temperature T (K). In addition, this expression allows the calculation of the Arrhenius constant A.

2.6 Error analysis

In order to find the model that best fits the experimental data, the coefficient of determination R^2 and 4 statistical errors were considered: the average standard percentage error ε (%), chi-square χ_i^2, sum of squared errors SSE, and sum of absolute errors SAE, described mathematically in Equations 15, 16, 17 and 18, respectively.

$$\varepsilon(\%) = \frac{1}{n}\sum\left|\frac{y_c - y_e}{y_e}\right| \tag{14}$$

$$\chi_i^2 = \sum \frac{(y_e - y_c)^2}{y_c} \qquad (15)$$

$$\mathbf{SSE} = \sum (y_e - y_c)^2 \qquad (16)$$

$$\mathbf{SAE} = \sum \left|(y_e - y_c)\right| \qquad (17)$$

The models were fitted using nonlinear regression in the minimization of χ_i^2, where, y_e is the experimental value, and y_c corresponds to the value calculated with the mathematical equation. The selection of the most appropriate model was based on the criteria of best fit and lowest recorded error. The Microsoft Office Excel program and the Solver optimization add-in[14,15] were used to process the data.

3. Results

3.1 Equilibrium studies, kinetics and thermodynamics

The graphical representation of the equilibrium models for TM-R40 is shown in **Figures 1a, 1b,** and **1c** at temperatures of 25 °C, 40 °C, and 55 °C.

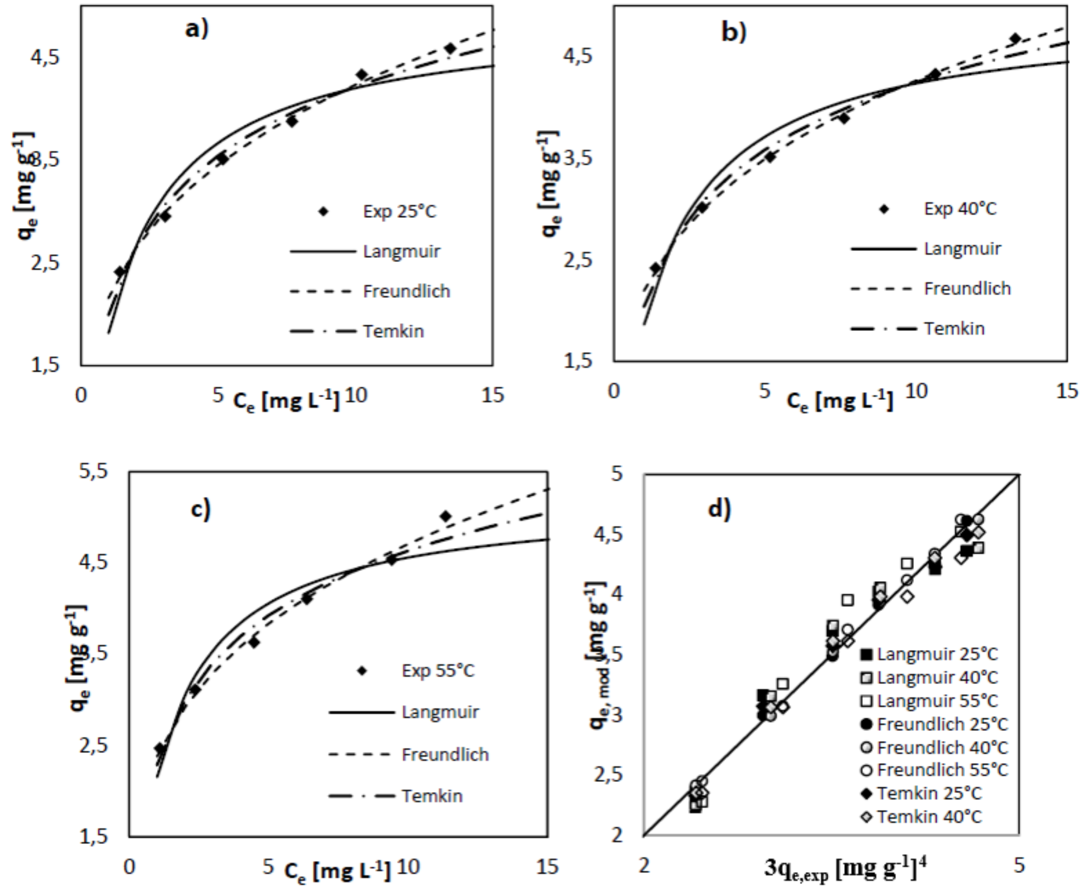

Figure 1. Representation of the models adjusted to the temperature. a): 25 °C; b): 40 °C; c): 55 °C and d): comparison of experimental and theoretical data.
Source: own elaboration

In the concentration range studied, an increasing behavior of the adsorbed charge and a concave curve towards the concentration axis, characteristic of the L-type in the isotherm classification proposed by Giles[16], where, in addition, a maximum adsorption limit is not evident. The comparison of the estimated values with the experimental values (**Figure 1d**) shows the magnitude of the deviation of each model as it moves away from the straight line. It is observed that the Langmuir model presents the greatest deviation, overestimating the load at medium concentrations and underestimating it at high concentrations. A similar effect is recorded for the Temkin model, but with a much smaller deviation, while the Freundlich model offers the best fit to the experimental data at all the temperatures and concentrations analyzed.

The parameters of each isotherm model are presented in **Table 1**. The error analysis points to the Freundlich isotherm as the most adequate model in the representation of the adsorption process equilibrium by possessing excellent correlations (R2 > 0.99) and low values in the average standard error percentage ($\varepsilon < 1.5\%$) at all temperatures evaluated. Likewise, the Temkin model, with R2 correlations greater than 0.97 and ε errors less than 3.0%, can represent isotherms acceptably. On the contrary, Langmuir obtained the lowest correlation and the highest error, discarding it as an adjustable model for the equilibrium of the TM-R40 system.

The ΔG° values were negative and show an increase in magnitude with increasing temperature. An R^2 correlation of 0.92 was reached for the regression of thermodynamic parameters with Equation 17, and positive values were found for ΔH° and ΔS° (**Table 1b**).

Table 1. Parameters of the fitted isotherm models: a) Langmuir, b) Freundlich, c) Temkin and d) thermodynamic parameters.

a) LANGMUIR

T [K]	q_{max} [mg g^{-1}]	K_L	R^2	χ_i^2	ε (%)	SSE	SAE
298	4.913	0.587	0.9432	0.0571	5.1743	0.1937	1.0565
313	4.933	0.607	0.9400	0.0580	4.9149	0.2107	1.0370
328	5.205	0.705	0.9244	0.0857	5.4766	0.3311	1.2052

b) FREUNDLICH

T [K]	K_F	N	R^2	χ_i^2	ε (%)	SSE	SAE
298	2.159	3.425	0.9970	0.0027	1.0283	0.0101	0.2233
313	2.197	3.474	0.9983	0.0015	0.6639	0.0059	0.1539
328	2.379	3.378	0.9929	0.0071	1.4712	0.0313	0.3600

c) TEMKIN

T [K]	A	B	R^2	χ_i^2	ε (%)	SSE	SAE
298	7.929	0.963	0.9857	0.0143	2.5891	0.0487	0.5311
313	8.371	0.959	0.9855	0.0133	2.2573	0.0511	0.4896
328	9.390	1.020	0.9748	0.0268	2.9161	0.1104	0.6714

d) Thermodynamic parameters

ΔG° (kJ mol^{-1})			ΔH° (kJ mol^{-1})	ΔS° (J mol^{-1} K^{-1})	R^2
T [K] 298	313	328			
-2.63	-2.85	-3.54	6.58	30.65	0.922

Source: own elaboration

Concerning the adsorption kinetics, a better fit was found for the three temperatures with the Ho pseudo-second-order model, by obtaining correlations close to 0.93 and such low errors ε less than 3.0% (**Table 2**). The value of the activation energy, Ea = 8.197 kJ·mol^{-1}, was determined from the second-order rate constant K2, by Equation 14. Its positive value corresponds to the expected character for this process[16].

The plots of the kinetic models for the TM-R40 system are presented in **Figures 2a**, **2b** and **2c**. That analyzed each of the temperatures. It is observed that the curve of the Ho pseudo-second-order model fits the experimental data very well, which confirms what was obtained from the error analysis. The other models present over and underestimations that reflect serious deviations. In general, the rapid occurrence of the process is noteworthy, since around 15 minutes at least 90 % of the entire load is reached at equilibrium, while the remaining value may require up to 60 minutes.

Table 2. Parameters of the kinetic models. a) Lagergren pseudo first order; b) Ho pseudo second order; c) Elovich; d) Activation energy

a) LAGERGREN							
T [K]	**K_1 [min^{-1}]**	**q_e [$mg\ g^{-1}$]**	**R^2**	**χ_i^2**	**ε (%)**	**SSE**	**SAE**
298	0.872	1.622	0.7017	0.0872	6.4653	0.1263	1.0301
313	0.987	1.616	0.7242	0.0635	5.1755	0.0949	0.8320
328	1.256	1.736	0.5538	0.0843	5.7953	0.1433	1.0342
b) HO							
T [K]	K_2 [$g\ mg^{-1}\ min^{-1}$]	q_e [$mg\ g^{-1}$]	R^2	χ_i^2	ε (%)	SSE	SAE
298	0.817	1.707	0.9544	0.0150	2.4379	0.0193	0.3720
313	0.968	1.693	0.9651	0.0091	1.7873	0.0120	0.2737
328	1.105	1.813	0.8835	0.0248	3.0049	0.0374	0.5154
c) ELOVICH							
T [K]	B	A [$mg\ g^{-1}$ min]	R^2	χ_i^2	ε (%)	SSE	SAE
298	7.732	1415.269	0.8575	0.0409	4.4392	0.0603	0.7261
313	8.698	5855.052	0.8335	0.0392	4.3561	0.0573	0.7094
328	7.970	5855.052	0.8652	0.0248	3.2316	0.0433	0.6102
D) ACTIVATION ENERGY							
K2 [$kJ\ mol^{-1}$]				Ea			
T [K] 298	313	328		[$kJ\ mol^{-1}$]		A	
0.817	0.968	1.105		8.197		22.414	

Source: own elaboration

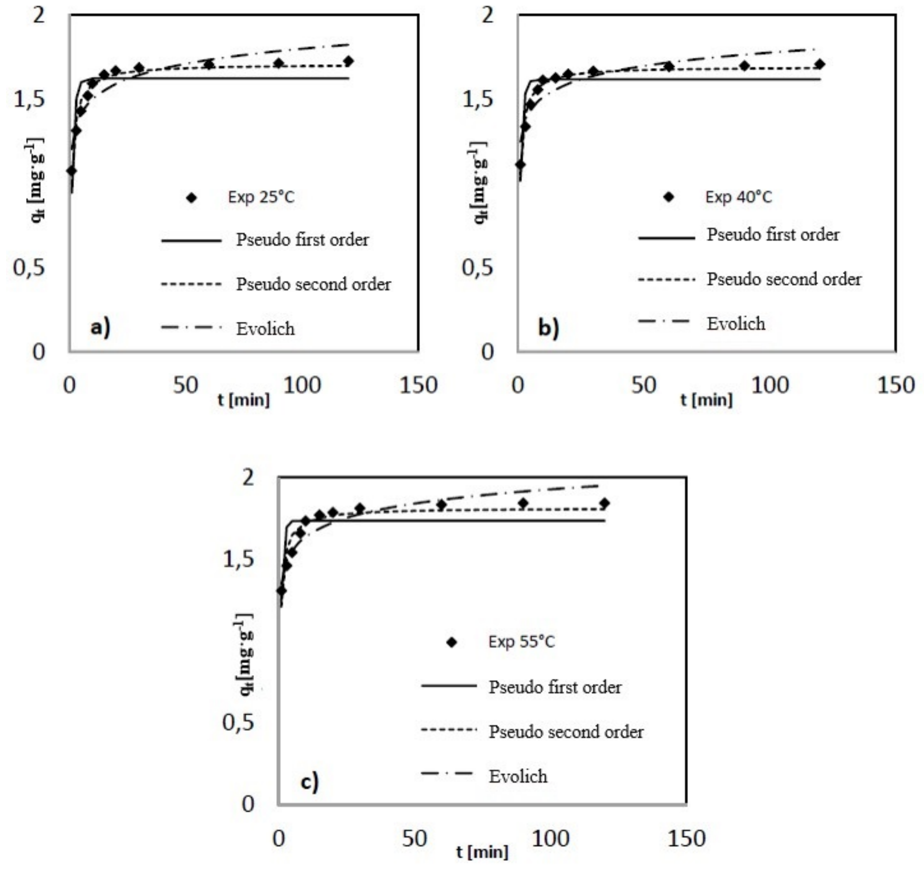

Figure 2. Models of the second order kinetics of the TM-R40 system adjusted to. a) 25 °C, b) 40 °C and c) 55 °C temperature.
Source: own elaboration

4. Discussion

For the equilibrium, an increase in the adsorbed charge at the respective concentration was observed with increasing temperature, this difference being more accentuated when going from 40 to 55 °C. This effect is best represented in the magnitude of the KF parameter, which indicates in a relative way the adsorption intensity. It can be seen that the increase of temperature leads to an increase in the value of this constant. Therefore, a higher loading of the dye on the adsorbent, especially at a given concentration. Similar results are described for dyes of anionic nature[17].

On the other hand, the value of n is much greater than unity at all temperatures evaluated, characteristic of concave curves towards the concentration axis, showing the favorability of the process. Furthermore, the increasing behavior in the isotherm suggests that adsorption occurs in multilayers with no apparent maximum adsorption limit; however, by using the Freundlich model to extrapolate an assumed loading of the dye at an R40 concentration of 1.0 $g \cdot L^{-1}$, this loading would be 18 $mg \cdot g^{-1}$, offering an indication of the loading expected at high concentrations.

Parameter A, corresponding to the maximum binding energy of the Temkin model, shows a remarkable increase with increasing temperature, while the value of parameter B, which indicates the heat of adsorption, does not show a clear trend, but has the highest value at the highest evaluated temperature of 55 °C. These two behaviors suggest the endothermic nature of the adsorption process[18]. The negative values obtained for $\Delta G°$ confirm the feasibility of the process and its spontaneous nature. On the contrary, the value of the enthalpy change, $\Delta H°$, was positive, pointing to the endothermic nature of the process. On the other hand, the positive value of $\Delta S°$ reflects the affinity of the adsorbent for the dye in the solution and some structural changes in the sorbate and adsorbent[2,9].

On the other hand, the pseudo-second-order Ho model showed a good fit and indicated that the estimated adsorption capacity increases with increasing temperature, an aspect that agrees with what was explained by the isotherm study. The kinetics obtained for the process is comparable to that of other acid dyes, both for the value of the constants and for its occurrence in the first 15 min with 90 % of the equilibrium load[19].

In particular, the value of the K2 constant presents an increase with increasing temperature, indicating that the speed of the process is favored as the temperature rises. The value obtained for the activation energy ($Ea = 8.197\ kJ \cdot mol^{-1}$), is in the range established for a process that takes place by physisorption[9,20], a nature that agrees with the pseudo-second-order kinetics criterion, with which the best correlation was found for the present study.

5. Conclusions

The equilibrium adsorption process of the TM-R40 couple is described by the Freundlich model, where the isotherms with their increasing behavior point to the formation of multilayers on the adsorbent, typical of adsorption systems of the TM-R40 couple.

Physical type. On the other hand, the kinetics is represented by the Ho pseudo-second-order model, where, in addition, its rapid occurrence offers advantages for further scaling developments. Finally, the negative value for the surface Gibbs free energy and the positive value for the entropy indicate the favorability and spontaneity of the process which, due to its endothermic character, is favored with increasing temperature. In short, the TM-R40 couple constitutes a suitable and feasible system to scale, since the adsorption process is spontaneous, endothermic with favored equilibrium and kinetics at high temperatures.

Acknowledgments

The authors express their gratitude to the National University of Colombia-Medellin Campus for the support for the infrastructure of the Experimental Chemistry Laboratory; likewise, to the Young Researchers and Innovators Program Year 2013, Call 617, for the financial support of the Project code 201010013080 and to the Research Vice-Rectory-National Directorate of Extension for the financing of the GTI project Code 40000001.

Conflict of interest

The authors declare that they have no conflict of interest.

References

1. Forgacs E, Cserháti T, Oros G. Emoval of synthetic dyes from wastewaters: a review. Environment International 2004; 30(7): 953–971.
2. Aksu Z, Tatlı Aİ, Tunç Ö. A comparative adsorption/biosorption study of Acid Blue 161: Effect of temperature on equilibrium and kinetic parameters.

Chemical Engineering Journal 2008; 142(1): 23–39.

3. Tripathi P, Srivastava VC, Kumar A. Optimization of an azo dye batch adsorption parameters using Box-Behnken design. Desalination 2009; 249(3): 1273–1279.
4. Soylak M, Unsal YE, Tuzen M. Spectrophotometric determination of trace levels of allura red in water samples after separation and preconcentration. Food and Chemical Toxicology 2011; 49(5): 1183–1187.
5. Crini G. Non-conventional low-cost adsorbents for dye removal: A review. Bioresource Technology 2006; 97(9): 1061–1185.
6. Brown D. Effects of colorants in the aquatic environment. Ecotoxicology and Environmental Safety 1987; 13(2):139–147.
7. Gupta VK, Suhas. Application of low-cost adsorbents for dye removal—A review. Journal of Environmental Management 2009; 90(8): 2313–2342.
8. Robinson T, Mcmullan G, Marchant R, *et al*. Remediation of dyes in textile effluent: a critical review on current treatment technologies with a proposed alternative. Bioresource Technology 2001; 77(3): 247–255.
9. Zheng L, Dang Z, Yi X, *et al*. Equilibrium and kinetic studies of adsorption of Cd (II) from aqueous solution using modified corn stalk. Journal of Hazardous Materials 2010; 176(1–3): 650–656.
10. Miretzky P, Cirelli aF. Cr (VI) and Cr (III) removal from aqueous solution by raw and modified lignocellulosic materials: A review. Journal of Hazardous Materials 2010; 180(1–3): 1–19.
11. Vadivelan V, Kumar KV. Equilibrium, kinetics, mechanism, and process design for the sorption of methylene blue onto rice husk. Journal of Colloid and Interface Science, 2005; 286(1): 90–100.
12. Ho YS, Chiu WT, Wang CC. Regression analysis for the sorption isotherms of basic dyes on sugarcane dust. Bioresource Technology 2005; 96(11): 1285–1291.
13. Tan IAW, Ahmad AL, Hameed BHH. Adsorption isotherms, kinetics, thermodynamics and desorption studies of 2, 4, 6-trichlorophenol on oil palm empty fruit bunch-based activated carbon. Journal of Hazardous Materials 2009; 164(2–3): 473–482.
14. Aksu Z, Isoglu IA. Use of agricultural waste sugar beet pulp for the removal of Gemazol turquoise blue-G reactive dye from aqueous solution. Journal of Hazardous Materials 2006; 137(1): 418–430.
15. Han R, Wang Y, Zou W, *et al*. Comparison of linear and nonlinear analysis in estimating the Thomas model parameters for methylene blue adsorption onto natural zeolite in fixed-bed column. Journal of Hazardous Materials 2007; 145(1–2): 331–335.
16. Limousin G, Gaudet JP, Charlet L, *et al*. Sorption isotherms: A review on physical bases, modeling and measurement. Applied Geochemistry 2007; 22(2): 249–275.
17. Yu L, Luo Y. The adsorption mechanism of anionic and cationic dyes by Jerusalem artichoke stalk-based mesoporous activated carbon. Journal of Environmental Chemical Engineering 2014; (2): 220–229.
18. Malana MA, Ijaz S, Ashiq MN. Removal of various dyes from aqueous media onto polymeric gels by adsorption process: Their kinetics and thermodynamics. Desalination 2010; 263(1–3): 249–257.
19. Arami M, Limaee NY, Mahmoodi NM, *et al*. Equilibrium and kinetics studies for the adsorption of direct and acid dyes from aqueous solution by soy meal hull. Journal of Hazardous Materials 2006; 135(1–3): 171–179.
20. Nollet H, Roels M, Lutgen P, *et al*. Removal of PCBs from wastewater using fly ash. Chemosphere 2003; 53(6): 655–665.